

Direct measurement of the branching fraction  
for the decay of  $D^+ \rightarrow \bar{K}^0 e^+ \nu_e$  and determination  
of  $\Gamma(D^0 \rightarrow K^- e^+ \nu_e) / \Gamma(D^+ \rightarrow \bar{K}^0 e^+ \nu_e)$

BES Collaboration

M. Ablikim<sup>a</sup>, J.Z. Bai<sup>a</sup>, Y. Ban<sup>j</sup>, J.G. Bian<sup>a</sup>, X. Cai<sup>a</sup>, J.F. Chang<sup>a</sup>, H.F. Chen<sup>o</sup>,  
H.S. Chen<sup>a</sup>, H.X. Chen<sup>a</sup>, J.C. Chen<sup>a</sup>, Jin Chen<sup>a</sup>, Jun Chen<sup>f</sup>, M.L. Chen<sup>a</sup>, Y.B. Chen<sup>a</sup>,  
S.P. Chi<sup>b</sup>, Y.P. Chu<sup>a</sup>, X.Z. Cui<sup>a</sup>, H.L. Dai<sup>a</sup>, Y.S. Dai<sup>q</sup>, Z.Y. Deng<sup>a</sup>, L.Y. Dong<sup>a</sup>,  
S.X. Du<sup>a</sup>, Z.Z. Du<sup>a</sup>, J. Fang<sup>a</sup>, S.S. Fang<sup>b</sup>, C.D. Fu<sup>a</sup>, H.Y. Fu<sup>a</sup>, C.S. Gao<sup>a</sup>, Y.N. Gao<sup>n</sup>,  
M.Y. Gong<sup>a</sup>, W.X. Gong<sup>a</sup>, S.D. Gu<sup>a</sup>, Y.N. Guo<sup>a</sup>, Y.Q. Guo<sup>a</sup>, K.L. He<sup>a</sup>, M. He<sup>k</sup>,  
X. He<sup>a</sup>, Y.K. Heng<sup>a</sup>, H.M. Hu<sup>a</sup>, T. Hu<sup>a</sup>, L. Huang<sup>f</sup>, X.P. Huang<sup>a</sup>, X.B. Ji<sup>a</sup>, Q.Y. Jia<sup>j</sup>,  
C.H. Jiang<sup>a</sup>, X.S. Jiang<sup>a</sup>, D.P. Jin<sup>a</sup>, S. Jin<sup>a</sup>, Y. Jin<sup>a</sup>, Y.F. Lai<sup>a</sup>, F. Li<sup>a</sup>, G. Li<sup>a</sup>, H.H. Li<sup>a</sup>,  
J. Li<sup>a</sup>, J.C. Li<sup>a</sup>, Q.J. Li<sup>a</sup>, R.B. Li<sup>a</sup>, R.Y. Li<sup>a</sup>, S.M. Li<sup>a</sup>, W.G. Li<sup>a</sup>, X.L. Li<sup>g</sup>, X.Q. Li<sup>i</sup>,  
X.S. Li<sup>n</sup>, Y.F. Liang<sup>m</sup>, H.B. Liao<sup>e</sup>, C.X. Liu<sup>a</sup>, F. Liu<sup>e</sup>, Fang Liu<sup>o</sup>, H.M. Liu<sup>a</sup>,  
J.B. Liu<sup>a</sup>, J.P. Liu<sup>p</sup>, R.G. Liu<sup>a</sup>, Z.A. Liu<sup>a</sup>, Z.X. Liu<sup>a</sup>, F. Lu<sup>a</sup>, G.R. Lu<sup>d</sup>, J.G. Lu<sup>a</sup>,  
C.L. Luo<sup>h</sup>, X.L. Luo<sup>a</sup>, F.C. Ma<sup>g</sup>, J.M. Ma<sup>a</sup>, L.L. Ma<sup>k</sup>, Q.M. Ma<sup>a</sup>, X.Y. Ma<sup>a</sup>,  
Z.P. Mao<sup>a</sup>, X.H. Mo<sup>a</sup>, J. Nie<sup>a</sup>, Z.D. Nie<sup>a</sup>, H.P. Peng<sup>o</sup>, N.D. Qi<sup>a</sup>, C.D. Qian<sup>l</sup>, H. Qin<sup>h</sup>,  
J.F. Qiu<sup>a</sup>, Z.Y. Ren<sup>a</sup>, G. Rong<sup>a</sup>, L.Y. Shan<sup>a</sup>, L. Shang<sup>a</sup>, D.L. Shen<sup>a</sup>, X.Y. Shen<sup>a</sup>,  
H.Y. Sheng<sup>a</sup>, F. Shi<sup>a</sup>, X. Shi<sup>j</sup>, H.S. Sun<sup>a</sup>, S.S. Sun<sup>o</sup>, Y.Z. Sun<sup>a</sup>, Z.J. Sun<sup>a</sup>, X. Tang<sup>a</sup>,  
N. Tao<sup>o</sup>, Y.R. Tian<sup>n</sup>, G.L. Tong<sup>a</sup>, D.Y. Wang<sup>a</sup>, J.Z. Wang<sup>a</sup>, K. Wang<sup>o</sup>, L. Wang<sup>a</sup>,  
L.S. Wang<sup>a</sup>, M. Wang<sup>a</sup>, P. Wang<sup>a</sup>, P.L. Wang<sup>a</sup>, S.Z. Wang<sup>a</sup>, W.F. Wang<sup>a</sup>, Y.F. Wang<sup>a</sup>,  
Zhe Wang<sup>a</sup>, Z. Wang<sup>a</sup>, Zheng Wang<sup>a</sup>, Z.Y. Wang<sup>a</sup>, C.L. Wei<sup>a</sup>, D.H. Wei<sup>c</sup>, N. Wu<sup>a</sup>,  
Y.M. Wu<sup>a</sup>, X.M. Xia<sup>a</sup>, X.X. Xie<sup>a</sup>, B. Xin<sup>g</sup>, G.F. Xu<sup>a</sup>, H. Xu<sup>a</sup>, Y. Xu<sup>a</sup>, S.T. Xue<sup>a</sup>,  
M.L. Yan<sup>o</sup>, F. Yang<sup>i</sup>, H.X. Yang<sup>a</sup>, J. Yang<sup>o</sup>, S.D. Yang<sup>a</sup>, Y.X. Yang<sup>c</sup>, M. Ye<sup>a</sup>,  
M.H. Ye<sup>b</sup>, Y.X. Ye<sup>o</sup>, L.H. Yi<sup>f</sup>, Z.Y. Yi<sup>a</sup>, C.S. Yu<sup>a</sup>, G.W. Yu<sup>a</sup>, C.Z. Yuan<sup>a</sup>, J.M. Yuan<sup>a</sup>,  
Y. Yuan<sup>a</sup>, Q. Yue<sup>a</sup>, S.L. Zang<sup>a</sup>, Yu. Zeng<sup>a</sup>, Y. Zeng<sup>f</sup>, B.X. Zhang<sup>a</sup>, B.Y. Zhang<sup>a</sup>,  
C.C. Zhang<sup>a</sup>, D.H. Zhang<sup>a</sup>, H.Y. Zhang<sup>a</sup>, J. Zhang<sup>a</sup>, J.Y. Zhang<sup>a</sup>, J.W. Zhang<sup>a</sup>,  
L.S. Zhang<sup>a</sup>, Q.J. Zhang<sup>a</sup>, S.Q. Zhang<sup>a</sup>, X.M. Zhang<sup>a</sup>, X.Y. Zhang<sup>k</sup>, Y.J. Zhang<sup>j</sup>,  
Y.Y. Zhang<sup>a</sup>, Yiyun Zhang<sup>m</sup>, Z.P. Zhang<sup>o</sup>, Z.Q. Zhang<sup>d</sup>, D.X. Zhao<sup>a</sup>, J.B. Zhao<sup>a</sup>,  
J.W. Zhao<sup>a</sup>, M.G. Zhao<sup>i</sup>, P.P. Zhao<sup>a</sup>, W.R. Zhao<sup>a</sup>, X.J. Zhao<sup>a</sup>, Y.B. Zhao<sup>a</sup>,

H.Q. Zheng<sup>j</sup>, J.P. Zheng<sup>a</sup>, L.S. Zheng<sup>a</sup>, Z.P. Zheng<sup>a</sup>, X.C. Zhong<sup>a</sup>, B.Q. Zhou<sup>a</sup>,  
G.M. Zhou<sup>a</sup>, L. Zhou<sup>a</sup>, N.F. Zhou<sup>a</sup>, K.J. Zhu<sup>a</sup>, Q.M. Zhu<sup>a</sup>, Y.C. Zhu<sup>a</sup>, Y.S. Zhu<sup>a</sup>,  
Yingchun Zhu<sup>a</sup>, Z.A. Zhu<sup>a</sup>, B.A. Zhuang<sup>a</sup>, B.S. Zou<sup>a</sup>

<sup>a</sup> Institute of High Energy Physics, Beijing 100039, People's Republic of China

<sup>b</sup> China Center for Advanced Science and Technology, Beijing 100080, People's Republic of China

<sup>c</sup> Guangxi Normal University, Guilin 541004, People's Republic of China

<sup>d</sup> Henan Normal University, Xinxiang 453002, People's Republic of China

<sup>e</sup> Huazhong Normal University, Wuhan 430079, People's Republic of China

<sup>f</sup> Hunan University, Changsha 410082, People's Republic of China

<sup>g</sup> Liaoning University, Shenyang 110036, People's Republic of China

<sup>h</sup> Nanjing Normal University, Nanjing 210097, People's Republic of China

<sup>i</sup> Nankai University, Tianjin 300071, People's Republic of China

<sup>j</sup> Peking University, Beijing 100871, People's Republic of China

<sup>k</sup> Shandong University, Jinan 250100, People's Republic of China

<sup>l</sup> Shanghai Jiaotong University, Shanghai 200030, People's Republic of China

<sup>m</sup> Sichuan University, Chengdu 610064, People's Republic of China

<sup>n</sup> Tsinghua University, Beijing 100084, People's Republic of China

<sup>o</sup> University of Science and Technology of China, Hefei 230026, People's Republic of China

<sup>p</sup> Wuhan University, Wuhan 430072, People's Republic of China

<sup>q</sup> Zhejiang University, Hangzhou 310028, People's Republic of China

Received 9 October 2004; accepted 10 December 2004

Available online 21 December 2004

Editor: M. Doser

## Abstract

The absolute branching fraction for the decay  $D^+ \rightarrow \bar{K}^0 e^+ \nu_e$  is determined using  $5321 \pm 149 \pm 160$  singly tagged  $D^-$  event sample from the data collected around 3.773 GeV with the BES-II detector at the BEPC collider. In the system recoiling against the singly tagged  $D^-$  mesons,  $34.4 \pm 6.1$  events for  $D^+ \rightarrow \bar{K}^0 e^+ \nu_e$  are observed. Those yield the absolute branching fraction to be  $BF(D^+ \rightarrow \bar{K}^0 e^+ \nu_e) = (8.95 \pm 1.59 \pm 0.67)\%$ . The ratio of the two partial widths for the decays of  $D^0 \rightarrow K^- e^+ \nu_e$  and  $D^+ \rightarrow \bar{K}^0 e^+ \nu_e$  is determined to be  $\Gamma(D^0 \rightarrow K^- e^+ \nu_e) / \Gamma(D^+ \rightarrow \bar{K}^0 e^+ \nu_e) = 1.08 \pm 0.22 \pm 0.07$ .

© 2004 Elsevier B.V. Open access under CC BY license.

## 1. Introduction

Experimental study of the exclusive semileptonic decays of the charged and neutral  $D$  mesons can provide important information of the decay mechanisms. Fig. 1(a) and (b) shows the decay diagrams of the  $D^0 \rightarrow K^- e^+ \nu_e$  and the  $D^+ \rightarrow \bar{K}^0 e^+ \nu_e$ , respectively. The isospin symmetry predicts that the partial widths of the two decay processes should be equal. However, the ratio of the two partial widths is

$$\frac{\Gamma(D^0 \rightarrow K^- e^+ \nu_e)}{\Gamma(D^+ \rightarrow \bar{K}^0 e^+ \nu_e)} = 1.34 \pm 0.20,$$

which is determined based on the measured branching fractions for the two decay processes and the lifetimes of the  $D^0$  and  $D^+$  quoted from PDG [1]. It deviates by  $1.7\sigma$  from the expected unit ratio.

To test the isospin symmetry in the exclusive semileptonic decays of the charged and neutral  $D$  mesons, we studied the two decay modes of  $D^0 \rightarrow K^- e^+ \nu_e$  [2] and  $D^+ \rightarrow \bar{K}^0 e^+ \nu_e$  with the same data sample of about  $33 \text{ pb}^{-1}$  collected at and around the center-of-mass energy of 3.773 GeV with the BES-II detector at

E-mail address: rongg@mail.ihep.ac.cn (G. Rong).

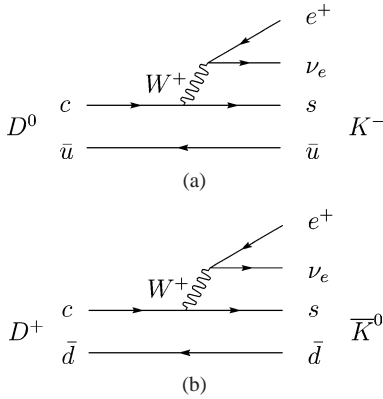


Fig. 1. The decay diagrams for (a)  $D^0 \rightarrow K^- e^+ \nu_e$  and (b)  $D^+ \rightarrow \bar{K}^0 e^+ \nu_e$ .

the BEPC collider. In this Letter, we report the direct measurements of the branching fraction for the decay of  $D^+ \rightarrow \bar{K}^0 e^+ \nu_e$  (throughout this Letter, charged conjugation is implied) and the ratio of the two decay widths.

## 2. The BES-II detector

The BES-II is a conventional cylindrical magnetic detector that is described in detail in Ref. [3]. A 12-layer vertex chamber (VC) surrounding the beryllium beam pipe provides input to the event trigger, as well as coordinate information. A forty-layer main drift chamber (MDC) located just outside the VC yields precise measurements of charged particle trajectories with a solid angle coverage of 85% of  $4\pi$ ; it also provides ionization energy loss ( $dE/dx$ ) measurements which are used for particle identification. Momentum resolution of  $1.7\% \sqrt{1 + p^2}$  ( $p$  in GeV/ $c$ ) and  $dE/dx$  resolution of 8.5% for Bhabha scattering electrons are obtained for the data taken at  $\sqrt{s} = 3.773$  GeV. An array of 48 scintillation counters surrounding the MDC measures the time of flight (TOF) of charged particles with a resolution of about 180 ps for electrons. Outside the TOF, a 12 radiation length, lead-gas barrel shower counter (BSC), operating in limited streamer mode, measures the energies of electrons and photons over 80% of the total solid angle with an energy resolution of  $\sigma_E/E = 0.22/\sqrt{E}$  ( $E$  in GeV) and spatial resolutions of  $\sigma_\phi = 7.9$  mrad and  $\sigma_Z = 2.3$  cm for electrons. A solenoidal magnet outside the BSC provides a 0.4 T magnetic field in the central tracking region of the de-

tector. Three double-layer muon counters instrument the magnet flux return, and serve to identify muons of momentum greater than 500 MeV/ $c$ . They cover 68% of the total solid angle.

## 3. Data analysis

Around the center of mass energy 3.773 GeV, the  $\psi(3770)$  resonance is produced in electron–positron ( $e^+e^-$ ) annihilation. The  $\psi(3770)$  decays predominantly into  $D\bar{D}$  pairs. If a  $D^-$  meson is fully reconstructed (this is called a singly tagged  $D^-$  meson), the  $D^+$  meson must exist in the system recoiling against the singly tagged  $D^-$  meson. Using the singly tagged  $D^-$  meson sample, the decay of  $D^+ \rightarrow \bar{K}^0 e^+ \nu_e$  can be well selected in the recoiling system. Therefore, the absolute branching fraction for the decay of  $D^+ \rightarrow \bar{K}^0 e^+ \nu_e$  can be well measured.

### 3.1. Events selection

The  $D^-$  meson is reconstructed in non-leptonic decay modes of  $K^+\pi^-\pi^-$ ,  $K^0\pi^-$ ,  $K^0K^-$ ,  $K^+K^-\pi^-$ ,  $K^0\pi^-\pi^-\pi^+$ ,  $K^0\pi^-\pi^0$ ,  $K^+\pi^-\pi^-\pi^0$ ,  $K^+\pi^+\pi^-\pi^-\pi^-$  and  $\pi^+\pi^-\pi^-$ . Events which contain at least three reconstructed charged tracks with good helix fits are selected. In order to ensure well-measured 3-momentum vectors and reliably charged particle identification, the charged tracks used in the single tag analysis are required to be within  $|\cos\theta| < 0.85$ , where  $\theta$  is the polar angle. All tracks, save those from  $K_S^0$  decays, must originate from the interaction region, which require that the closest approach of a charged track in the  $xy$  plane is less than 2.0 cm and the  $z$  position of the charged track is less than 20.0 cm. Pions and kaons are identified by means of TOF and  $dE/dx$  measurements. Pion identification requires a consistency with the pion hypothesis at a confidence level ( $CL_\pi$ ) greater than 0.1%. In order to reduce misidentification, a kaon candidate is required to have a larger confidence level ( $CL_K$ ) for a kaon hypothesis than that for a pion hypothesis. For electron identification, the combined confidence level ( $CL_e$ ), calculated for the  $e$  hypothesis using the  $dE/dx$ , TOF and BSC measurements, is required to be greater than 0.1%, and the ratio  $CL_e/(CL_e + CL_\pi + CL_K)$  is required to be greater than 0.8. The  $\pi^0$  is reconstructed in the decay of  $\pi^0 \rightarrow \gamma\gamma$ . To select good photons from the decay of

$\pi^0$ , the energy of a photon deposited in the BSC is required to be greater than 0.07 GeV [2], and the electromagnetic shower is required to start in the first 5 read-out layers. In order to reduce backgrounds the angle between the photon and the nearest charged track is required to be greater than  $22^\circ$  [2] and the angle between the direction of the cluster development and the direction of the photon emission to be less than  $37^\circ$  [2].

For the single tag modes of  $D^- \rightarrow K^+\pi^+\pi^-\pi^-\pi^-$  and  $D^- \rightarrow \pi^+\pi^-\pi^-$ , backgrounds are further reduced by requiring the difference between the measured energy of the  $D^-$  candidate and the beam energy to be less than 70 and 60 MeV, respectively. In addition, the cosine of the  $D^-$  production angle relative to the beam direction is required to be  $|\cos\theta_{D^-}| < 0.8$ .

### 3.2. Singly tagged $D^-$ sample

For each event, there may be several different charged track (or charged and neutral track) combinations for each of the nine single tag modes. Each combination is subject to a one-constraint (1C) kinematic fit requiring overall event energy conservation and that the unmeasured recoil system has the same invariant mass as the track combinations. Candidates with a fit probability  $P(\chi^2)$  greater than 0.1% are retained. If more than one combination satisfies  $P(\chi^2) > 0.1\%$ , the combination with the largest fit probability is retained. For the single tag modes with a neutral kaon and/or neutral pion, one additional constraint kinematic fit for the  $K_S^0 \rightarrow \pi^+\pi^-$  and/or  $\pi^0 \rightarrow \gamma\gamma$  hypothesis is performed, separately.

The resulting distributions in the fitted invariant masses of  $mKn\pi$  ( $m = 0$  or  $1$  or  $2$  and  $n = 1$  or  $2$  or  $3$  or  $4$ ) combinations, which are calculated using the fitted momentum vectors from the kinematic fit, are shown in Fig. 2. The signals for the singly tagged  $D^-$  mesons are clearly observed in the fitted mass spectra. A maximum likelihood fit to the mass spectrum with a Gaussian function for the  $D^-$  signal and a special background function<sup>1</sup> to describe back-

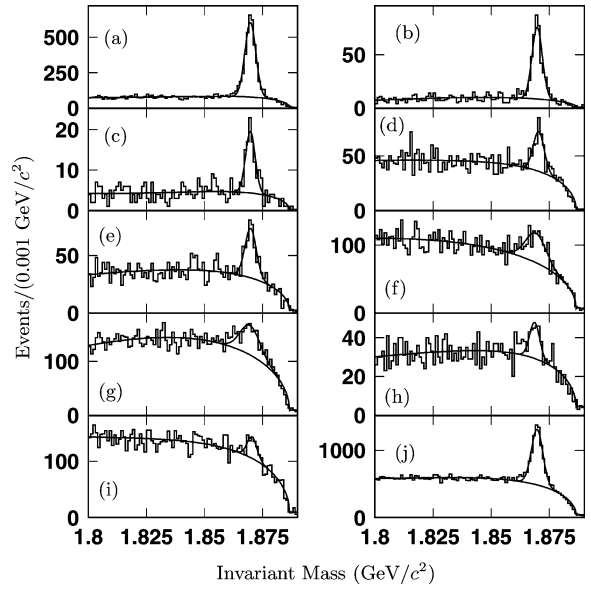


Fig. 2. The distributions of the fitted masses of (a)  $K^+\pi^-\pi^-$ , (b)  $K^0\pi^-$ , (c)  $K^0K^-$ , (d)  $K^+K^-\pi^-$ , (e)  $K^0\pi^-\pi^-\pi^+$ , (f)  $K^0\pi^-\pi^0$ , (g)  $K^+\pi^-\pi^-\pi^0$ , (h)  $K^+\pi^+\pi^-\pi^-\pi^-$ , and (i)  $\pi^-\pi^-\pi^+$  combinations; (j) is the fitted masses of the  $mKn\pi$  combinations for the 9 modes combined together.

grounds yields the number of the singly tagged  $D^-$  events for each of the nine modes and the total number of  $5321 \pm 149 \pm 160$  reconstructed  $D^-$  mesons, where the first error is statistical and the second systematic obtained by varying the parameterization of the background. The curves of Fig. 2 give the best fits to the invariant mass spectra. In the fits to the mass spectra, the standard deviations of the Gaussian signal functions for the Fig. 2(g) and (h) are fixed at 4.27 and 2.16 MeV, respectively. These standard deviations are obtained from Monte Carlo sample. All other parameters are left free in the fit.

### 3.3. Candidates of $D^+ \rightarrow \bar{K}^0 e^+ \nu_e$

Candidate events of the decay  $D^+ \rightarrow \bar{K}^0 e^+ \nu_e$  are selected from the surviving tracks in the system re-

<sup>1</sup> A Gaussian function was assumed for the signal. The background shape was

$$(1.0 + p_1 y + p_2 y^2) N \sqrt{1 - \left(\frac{x}{E_b}\right)^2} x e^{-f(1 - \frac{x}{E_b})^2} + c,$$

where  $N \sqrt{1 - (\frac{x}{E_b})^2} x e^{-f(1 - \frac{x}{E_b})^2}$  is the ARGUS background shape,  $x$  is the fitted mass,  $E_b$  is the beam energy,  $y = (E_b - x)/(E_b - 1.8)$ ,  $N$ ,  $f$ ,  $p_1$ ,  $p_2$  and  $c$  are the fit parameters. The parameter  $c$  accounts for the varying of the beam energy. The ARGUS background shape was used by the ARGUS experiment to parameterize the background for fitting  $B$  mass peaks. For details, see [4].

coiling against the tagged  $D^-$ . To select the  $D^+ \rightarrow \bar{K}^0 e^+ \nu_e$ , it is required that there are three charged tracks, one of which is identified as an electron with charge opposite to the charge of the tagged  $D^-$  and the other two as  $\pi^+$  and  $\pi^-$ . The difference between the invariant masses of the  $\pi^+ \pi^-$  combinations and the mass of  $K_S^0$  should be less than  $20 \text{ MeV}/c^2$ . The neutrino is undetected, therefore the kinematic quantity  $U_{\text{miss}} \equiv E_{\text{miss}} - p_{\text{miss}}$  is used to obtain the information about the missing neutrino, where  $E_{\text{miss}}$  and  $p_{\text{miss}}$  are the total energy and the total momentum of all missing particles respectively, which are carried by the undetected particles. The backgrounds from the decays such as  $D^+ \rightarrow \bar{K}^0 \pi^+ \pi^0$  and  $D^+ \rightarrow \bar{K}^0 \pi^0 e^+ \nu_e$  are suppressed by rejecting the events with extra isolated photons which are not used in the reconstruction of the singly tagged  $D^-$  meson. The isolated photon should have its energy greater than  $0.1 \text{ GeV}$  [2] and satisfy photon selection criteria as mentioned earlier.

Fig. 3 shows the  $U_{\text{miss}}$  distributions for the Monte Carlo  $D^+ \rightarrow \bar{K}^0 e^+ \nu_e$  events. The quantity  $U_{\text{miss}}$  is close to zero as expected. Fig. 4 shows the  $U_{\text{miss}}$  distribution for the events from the data, which satisfy the selection criteria. From the distribution, most of the events can be identified as the candidates of  $D^+ \rightarrow \bar{K}^0 e^+ \nu_e$  versus the tagged  $D^-$  mesons. Those can be further confirmed as follows. If we select the events which satisfy the requirement  $|U_{\text{miss},i}| < 3\sigma_{U_{\text{miss},i}}$  for the single tag mode( $i$ ), where  $\sigma_{U_{\text{miss},i}}$  is the standard deviation of the  $U_{\text{miss},i}$  distribution obtained from Monte Carlo simulation for the event of  $D^+ \rightarrow \bar{K}^0 e^+ \nu_e$  versus the single tag mode( $i$ ) ( $i = 1$  is for  $K^+ \pi^- \pi^-$ ;  $i = 2$  is for  $K^0 \pi^- \dots$  and  $i = 9$  is for  $\pi^+ \pi^- \pi^-$  modes), and plot the fitted masses of the  $mKn\pi$  combinations, we observe a clear signal of  $D^+ \rightarrow \bar{K}^0 e^+ \nu_e$  versus the  $D^-$  tags as shown in Fig. 5. In Fig. 5, there are 37 events in the  $\pm 3\sigma_{\text{mass},i}$  signal regions, while there are 4 events in the outside of the signal regions; where the  $\sigma_{\text{mass},i}$  is the standard deviation of the fitted mass distribution for the single tag mode( $i$ ). By assuming that the background distribution is flat,  $0.8 \pm 0.4$  background events are estimated in the signal region. There may also be the  $\pi^+ \pi^-$  combinatorial background. By selecting the events in which the invariant masses of the  $\pi^+ \pi^-$  combinations in the recoil side of the tags are outside of the  $K_S^0$  mass window, we estimate that there are  $0.3 \pm 0.2$  back-

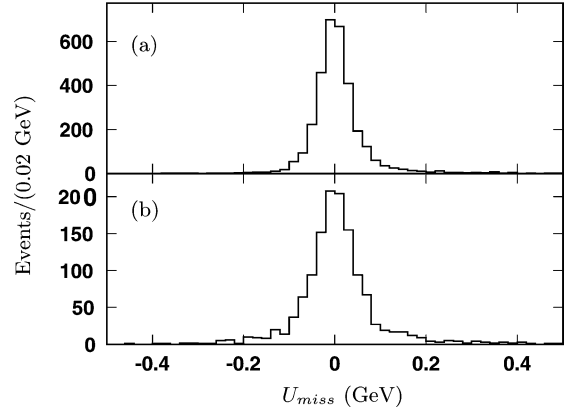


Fig. 3. The distributions of  $U_{\text{miss}}$  calculated for the Monte Carlo events of (a)  $D^+ \rightarrow \bar{K}^0 e^+ \nu$  versus  $D^- \rightarrow K^+ \pi^- \pi^-$  and (b)  $D^+ \rightarrow \bar{K}^0 e^+ \nu$  versus  $D^- \rightarrow K^+ \pi^- \pi^- \pi^0$ .

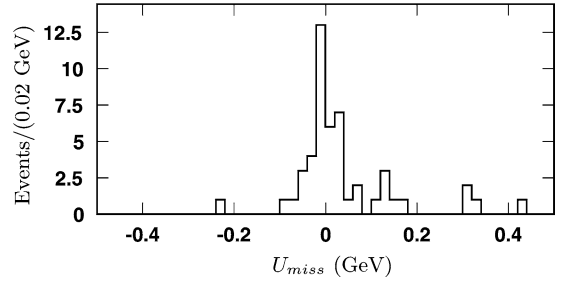


Fig. 4. The distribution of  $U_{\text{miss}}$  calculated for the selected events of  $D^+ \rightarrow \bar{K}^0 e^+ \nu$  versus  $D^-$  tags ( $mKn\pi$  combinations).

ground events in the candidate events. After subtracting these numbers of background events,  $35.9 \pm 6.1$  candidate events are retained.

The distribution of the momentum of the electrons from the selected candidate events of  $D^+ \rightarrow \bar{K}^0 e^+ \nu_e$  is shown in Fig. 6, where the error bars are for the events from the data and the histogram is for the events of  $D^+ \rightarrow \bar{K}^0 e^+ \nu_e$  from Monte Carlo sample. The measured electron momentum is in good agreement with the electron momentum from the Monte Carlo events of  $D^+ \rightarrow \bar{K}^0 e^+ \nu_e$ .

### 3.4. Background subtraction

There are still some background contaminations in the observed candidate events due to other semileptonic or hadronic decays. These background events must be subtracted from the candidate events. The

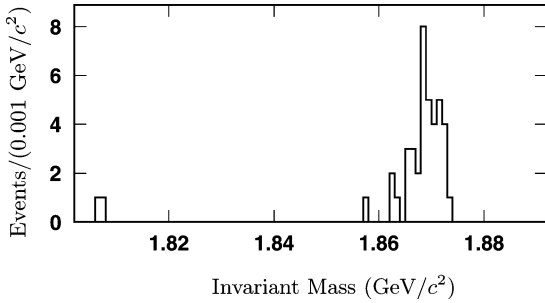


Fig. 5. The distribution of the fitted invariant masses of  $mK\bar{n}\pi$  combinations for the events in which the  $D^+ \rightarrow \bar{K}^0 e^+ \nu_e$  candidate events are observed in the system recoiling against the  $mK\bar{n}\pi$  combinations; where a clear signal for the singly tagged  $D^-$  is observed.

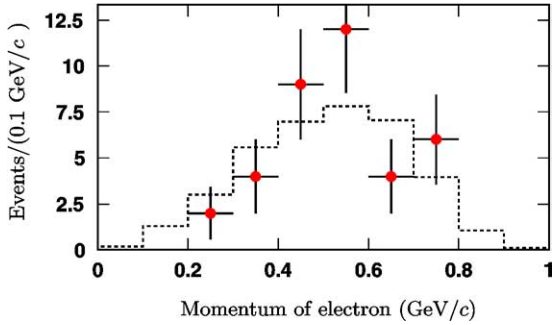


Fig. 6. The distribution of the momentum of the electrons from the selected candidate events of  $D^+ \rightarrow \bar{K}^0 e^+ \nu_e$ , where the error bars are for the events from the data and the histogram is for the events of  $D^+ \rightarrow \bar{K}^0 e^+ \nu_e$  from the Monte Carlo sample.

numbers of background events are estimated by analyzing the Monte Carlo sample which is 13 times larger than the data. The Monte Carlo events are generated as  $e^+e^- \rightarrow D\bar{D}$  and the  $D$  and  $\bar{D}$  mesons are set to decay to all possible final states according to the decay modes and branching fractions quoted from PDG [1] excluding the decay mode under study. The number of events satisfying the selection criteria is then renormalized to the corresponding data set. Totally  $1.5 \pm 0.4$  background events are obtained for  $D^+ \rightarrow \bar{K}^0 e^+ \nu_e$ . After subtracting the number of background events,  $34.4 \pm 6.1$  signal events for  $D^+ \rightarrow \bar{K}^0 e^+ \nu_e$  decay are retained.

Table 1

Comparison of our measured branching fraction for the decay of  $D^+ \rightarrow \bar{K}^0 e^+ \nu_e$  with that measured by MARK-III

Branching fraction (%) (this experiment)	Branching fraction (%) (MARK-III)
$8.95 \pm 1.59 \pm 0.67$	$6.0^{+2.2}_{-1.3} \pm 0.7$

## 4. Results

### 4.1. Monte Carlo efficiency

The efficiency for reconstruction of the semileptonic decay events of  $D^+ \rightarrow \bar{K}^0 e^+ \nu_e$  is estimated by Monte Carlo simulation. A detailed Monte Carlo study gives the efficiency to be  $\epsilon_{\bar{K}^0 e^+ \nu_e} = (7.22 \pm 0.06)\%$ , where the error is statistical.

### 4.2. Branching fraction

The measured branching fraction is obtained by dividing the observed number of the semileptonic decay events  $N(D^+ \rightarrow \bar{K}^0 e^+ \nu_e)$  by the number of the singly tagged  $D^-$  mesons  $N_{D_{\text{tag}}^-}$  and the reconstruction efficiency  $\epsilon_{\bar{K}^0 e^+ \nu_e}$ ,

$$Br(D^+ \rightarrow \bar{K}^0 e^+ \nu_e) = \frac{N(D^+ \rightarrow \bar{K}^0 e^+ \nu_e)}{\epsilon_{\bar{K}^0 e^+ \nu_e} \times N_{D_{\text{tag}}^-}}. \quad (1)$$

Inserting these numbers into Eq. (1), the branching fraction for  $D^+ \rightarrow \bar{K}^0 e^+ \nu_e$  decay is obtained to be

$$BF(D^+ \rightarrow \bar{K}^0 e^+ \nu_e) = (8.95 \pm 1.59 \pm 0.67)\%,$$

where the first error is statistical and the second systematic. The systematic uncertainty in the measured branching fraction arises from the particle identification (1.5%), tracking efficiency (2.0% per track), photon reconstruction (2.0%),  $U_{\text{miss}}$  selection (0.6%), the number of the singly tagged  $D^-$  mesons (3.0%), background subtraction (1.6%), Monte Carlo statistics (0.7%) and  $K_S^0$  selection (1.1%). These uncertainties are added in quadrature to obtain the total systematic error, which is 7.5%.

Table 1 gives the comparison of our measured value of the branching fraction for the decay of  $D^+ \rightarrow \bar{K}^0 e^+ \nu_e$  with that measured by MARK-III [5]. Our



measured branching fraction is consistent within the error with that measured by MARK-III.

#### 4.3. The ratio of $\frac{\Gamma(D^0 \rightarrow K^- e^+ \nu_e)}{\Gamma(D^+ \rightarrow \bar{K}^0 e^+ \nu_e)}$

With the same data sample, BES-II measured the absolute branching fraction for  $D^0 \rightarrow K^- e^+ \nu_e$  decay to be  $BF(D^0 \rightarrow K^- e^+ \nu_e) = (3.82 \pm 0.40 \pm 0.27)\%$  [2]. Using the measured branching fractions for the decays of  $D^0 \rightarrow K^- e^+ \nu_e$  and  $D^+ \rightarrow \bar{K}^0 e^+ \nu_e$  and the lifetimes of the  $D^0$  and  $D^+$  quoted from the PDG [1], the ratio of the decay widths is obtained to be

$$\frac{\Gamma(D^0 \rightarrow K^- e^+ \nu_e)}{\Gamma(D^+ \rightarrow \bar{K}^0 e^+ \nu_e)} = 1.08 \pm 0.22 \pm 0.07,$$

where the first error is statistical and the second systematic which arises from some uncanceled systematic uncertainty (6.8%) in the measured ratio of the branching fractions for the two decay modes and the uncertainty (0.8%) in the measured ratio of the  $D^0$  and  $D^+$  lifetimes [1].

## 5. Summary

In summary, by analyzing the data sample of about  $33 \text{ pb}^{-1}$  collected at and around 3.773 GeV with the BES-II detector at the BEPC collider, the branching fraction for the decay of  $D^+ \rightarrow \bar{K}^0 e^+ \nu_e$  has been measured. From a total of  $5321 \pm 149 \pm 160$  singly tagged  $D^-$  event sample,  $34.4 \pm 6.1$   $D^+ \rightarrow \bar{K}^0 e^+ \nu_e$  signal events are observed in the system recoiling against the singly tagged  $D^-$  mesons. Those yield the decay branching fraction to be  $BF(D^+ \rightarrow \bar{K}^0 e^+ \nu_e) = (8.95 \pm 1.59 \pm 0.67)\%$ . Using the values of the measured branching fractions for the decays of  $D^0 \rightarrow K^- e^+ \nu_e$  and  $D^+ \rightarrow \bar{K}^0 e^+ \nu_e$ , the ratio of the two par-

tial decay widths is determined to be

$$\frac{\Gamma(D^0 \rightarrow K^- e^+ \nu_e)}{\Gamma(D^+ \rightarrow \bar{K}^0 e^+ \nu_e)} = 1.08 \pm 0.22 \pm 0.07,$$

which is consistent within the errors with the theoretical prediction of the spectator model and supports that isospin conservation holds in the exclusive semi-leptonic decays of the  $D^+ \rightarrow \bar{K}^0 e^+ \nu_e$  and the  $D^0 \rightarrow K^- e^+ \nu_e$ .

## Acknowledgements

The BES Collaboration thanks the staff of BEPC for their hard efforts. This work is supported in part by the National Natural Science Foundation of China under contracts Nos. 19991480, 10225524, 10225525, the Chinese Academy of Sciences under contract No. KJ 95T-03, the 100 Talents Program of CAS under Contract Nos. U-11, U-24, U-25, and the Knowledge Innovation Project of CAS under Contract Nos. U-602, U-34 (IHEP); by the National Natural Science Foundation of China under Contract No. 10175060 (USTC), and No. 10225522 (Tsinghua University).

## References

- [1] Particle Data Group, S. Eidelman, et al., Phys. Lett. B 592 (2004) 1.
- [2] BES Collaboration, M. Ablikim, et al., Phys. Lett. B 597 (2004) 39, hep-ex/0406028.
- [3] BES Collaboration, J.Z. Bai, et al., Nucl. Instrum. Methods A 458 (2001) 627.
- [4] I.C. Brock, Mn-Fit, a fitting and plotting package using MINUIT, Version 4.07, 22 December 2000.
- [5] MARK-III Collaboration, Z. Bai, et al., Phys. Rev. Lett. 66 (1991) 1011.